Performance of Aeronautical Mobile Airport Communications System in the Case of Aircraft at Final Approaching or Initial Climbing

Yuchu Ji [1], Yang Wang [2], and Yuan Sang [3]

[1] College of Electronic Information and Automation
Civil Aviation University of China, Tianjin 300300, China
jiyuchu@126.com

[2] Tianjin Key Lab for Advanced Signal Processing
Civil Aviation University of China, Tianjin, 300300, China
raynor63@163.com

[3] Inventec Group (Tianjin) Electronic Technology Co. LTD, Tianjin, 300070, China
dorisbps@163.com

Abstract ― The aeronautical mobile airport communications system (AeroMACS) is proposed to support the communications between the tower and aircrafts or the service vehicles in the range of airport. In this paper, the working environment that the aircraft at final approaching or initial climbing (AFAIC) is researched. By considering the influence of Doppler frequency shift and the channel model in AFAIC case, we propose a transmission scheme which can obtain preferable transmission performance for low order modulation. Simulation results of the signal-to-noise ratio loss, the spectrum efficiency and the bit error rate are given, which indicate that the proposed scheme can meet the demand of AeroMACS and expand the zone of airport communication area.

Index Terms ― Aeronautical mobile airport communications system, communication in aircraft at final approaching and initial climbing case, signal processing.

I. INTRODUCTION

The increase of air traffic in civil airports has led to a growth of data loads needed for both air traffic control (ATC) and airline operational communications (AOC) services. The new generation of air traffic management (ATM) system needs the support of a broadband communication structure able to satisfy the increasing application and service requirements foreseen by the Communications Operating Concept and Requirements (COCR) [1].

To satisfy the communication order, both international civil aviation organization (ICAO) and Eurocontrol identified a solution to provide dedicated aeronautical communications on the airport surface. This system is named aeronautical mobile airport communications system (AeroMACS), which supports the aircraft are in closest proximity to each other and to a wide variety of service and operational support aircrafts, vehicles, personnel, and infrastructures [2,3]. AeroMACS is based on the IEEE 802.16e standard, known as Mobile WiMAX [4].

The AeroMACS operates in the aeronautical C-band, which is with the frequency between 5091 MHz and 5150 MHz, and divided into 11 separated subchannels with the bandwidth of 5MHz. The transmission characteristics and the antenna design of the aeronautical C-band has been widely studied [5,6]. In particular, non-line-of-sight (NLoS) communications are supported by means of orthogonal frequency division multiplexing access (OFDMA) technology, which provides robustness against detrimental propagation effects and efficient use of resources, thus enabling high-data-rate services.

According to the AeroMACS profile, OFDMA frames follow a time division duplexing (TDD) structure, in which the downlink (DL) and uplink (UL) transmissions occur at different times and share the same frequency channel, and the AeroMACS frame occupies the entire 5 MHz channel during its 5 milliseconds duration.

In [2] and [3], the concept and the basic scheme of AeroMACS is introduced. The transmission efficiency and performance is analyzed in [4] and [7]. The typical transmission case, which considers different communication environment and variety kind of access node (i.e., aircrafts, vehicles and sensors), is discussed in [8]. The MIMO antenna configuration scheme is proposed and tested in [9] and [10], and the multi-hop relay scheme based on IEEE 802.16j is proposed in [11].

Submitted On: January 1, 2020
Accepted On: May 4, 2020

To describe different work environments in the airport, two typical working cases, the aircraft at hangar taxiway or runway (AHTR) and the aircraft at the gate (AG) are defined [8]. In AHTR case, there is few obstacles between the access nodes, and the channels between different nodes contain one LOS path and some NLOS paths. In AG case, there are several aircrafts and tens of vehicles in one communication cell, and the channels between different nodes do not have LOS path.

Beside the two abovementioned cases, aircraft at final approaching or initial climbing (AFAIC) progress plays an important part of ATM communication in AeroMACS. The aircraft operation data in AFAIC case is also important to realizing the high level advanced surface movement guidance and control system (A-SMGCS) or the automatic aircraft navigation such as automatic approaching or landing.

In AFAIC case, high approaching or climbing speed of aircraft leads to strong Doppler frequency shift in the communication system, which leads to intersubcarrier interference of the OFDMA scheme. Besides, the communication channel in the AFAIC case is with strong LOS path, which is different from the AG and AHTR cases.

To improve the transmission performance, many intersubcarrier interference cancellation schemes and transmission schemes are proposed [12-15]. In [16], a Doppler shift and timing error estimation and cancellation scheme is proposed for AeroMACS. However, it is with complicated decoding process, and the special channel between the base station and the aircraft in AFAIC case has not been considered.

In this paper, the transmission mode of AFAIC case in AeroMACS has been researched. By considering the influence of Doppler frequency shift and the channel model in AFAIC case, we propose a transmission scheme that the decoding process is similitude with the existing one in IEEE 802.16e. It is easy to be realized during the construction process of AeroMACS. Simulation results of the signal-to-noise ratio (SNR) loss, the spectrum efficiency and the bit error rate (BER) are also given at the end of this paper.

II. SYSTEM MODEL

As shown in Fig. 1, the AeroMACS network architecture is based on IEEE 802.16e [17], which is an all-IP network that decouples the access architecture from IP connectivity and allows modularity and flexibility.

The mobile station (MS) and the subscriber station (SS) are the end user devices. The MS nodes are moving nodes such as aircrafts, vehicles, and personal nodes in the airport. The SS nodes are fixed nodes such as radar, weather stations, and sensors in the movement area of the airport.

The base station (BS) is the access point to the network, implementing air interface and the access functionalities including UL and DL scheduler, radio resource management, and handover (HO) control. Each BS operates on an angular sector and is at a given frequency. During different transmission environments, the cover area of BS can be large (e.g., the macro cell for the AHTR scenery) or small (e.g., the micro cell for the AG scenery).

Access service network (ASN) is in charge of all the functions needed to provide radio access to AeroMACS subscriber, authentication, and resource management procedures. The connectivity service network (CSN) is a set of network functions that provide IP connectivity services to the AeroMACS subscriber. The ASN gateway, represents the link between the ASN and the CSN, described below, performing routing or bridging functions.

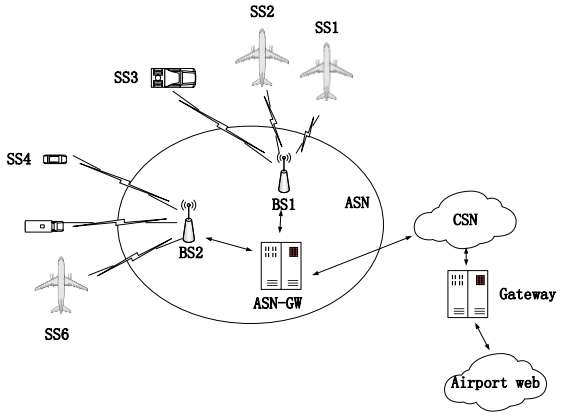

Fig. 1. Typical AeroMACS network, which includes BS node, MS nodes and SS nodes. The ASN, CSN and the ASN gateway realize the connection to the airport web.

In AFAIC case, the aircraft approaches to or climbs from the runway with the similar track. Considering that the minima taking-off interval or approaching interval in civil ATC rule is about 10 km, and the cover range of BS in macro cell reaches more than 10 km, as shown in Fig. 2, the number of MS node in AFAIC is limited (Normally, BS covers 2 aircrafts during both approaching and climbing cases).

Since the approaching speed or the climbing speed of aircraft is a dynamic value, which affected by aircraft type, load, oil quantity and wind speed, in [18], five categories, i.e., CAT A, B, C, D and E, of typical aircraft have been established by different approaching speed. In general, for normal civil aircraft, the speed range of AFAIC case is between 200km/h (kilometers per hour) and 400km/h [15]. The channel between BS and MS in AFAIC scenery is the fast fading channel with strong Doppler frequency shift. In the OFDM system, we take ε as the normalized offset frequency:

$$\varepsilon = Nf_c T_S v/c\,, \tag{1}$$

where f_c is the carrier frequency, c is the light speed, and v is the moving speed of MS in meter per second, N is the number of the DFT point in OFDMA scheme and T_S is the symbol period duration time.

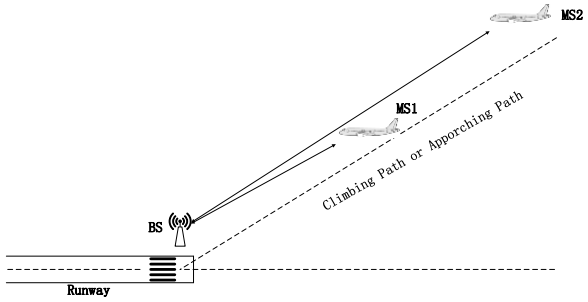

Fig. 2. The AFAIC case. The aircrafts are approaching or climbing with the similar track.

In the typical AeroMACS, considering the above-mentioned speed range in AFAIC case, and assuming that the carrier frequency is 5GHz, the number of DFT point is 512, and the symbol period duration time is 1.75×10^{-7} seconds, the range of ε is:

$$\varepsilon \in \left[4.97\times10^{-2}, 1.66\times10^{-1}\right]. \tag{2}$$

The channel model of AFAIC case is shown in Fig. 3, which is with one LOS path and some NLOS paths, and it is a typical Rice model.

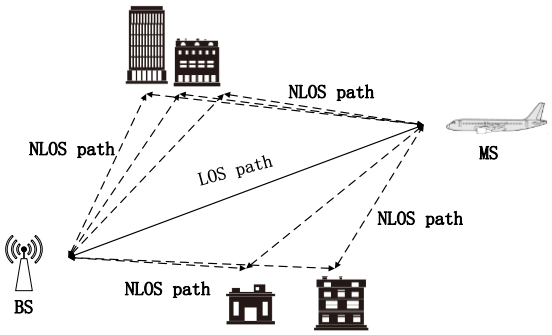

Fig. 3. Channel model of AFAIC case, which contains one LOS path and several NLOS paths.

Define the amplitude of the LOS path is a, the variance of the diffuse process with zero-mean quadrature components of NLOS path is c, The Rice factor, which is the power ratio between the LOS and the diffuse components is given by:

$$K_{\mathrm{RICE}} = 10\lg\left(\frac{a^2}{c^2}\right)\mathrm{dB}\,. \tag{3}$$

Define the number of NLOS path is N. Let f_D and be the Doppler shifting frequency of the LOS path. The phase shift, the Doppler shifting frequency and the time delay of the n-th NLOS path are θ_n, f_{D_n} and τ_n, respectively. The channel function of AFAIC is given by:

$$h(t) = ae^{j2\pi f_D t} + c\frac{1}{\sqrt{N}}\sum_{n=1}^{N} e^{j\theta_n} e^{j2\pi f_{Dn} t} e^{-j2\pi\tau_n}\,. \tag{4}$$

In (4), $ae^{j2\pi f_D t}$ denotes the channel function of the LOS path, and the rest parts denote the channel function of the NLOS paths where $e^{j\theta_n}$, $e^{j2\pi f_{Dn}}$ and $e^{-j2\pi\tau_n}$ represent the phase shifting component, the Doppler shift component and the time delay heft component of the n-th NLOS path, respectively.

As discussed in [15], in the typical AFAIC case, the parameter K_{RICE} is between 9dB and 20dB, and the typical value of K_{RICE} is 15dB. The typical number of NLOS path is 20.

III. TRANSMISSION MODEL IN AFAIC CASE

From the physical layer specifications, the DL of OFDMA scheme is essentially equivalent to an OFDM system that in one symbol period, BS can occupy the all subcarriers. Let $\boldsymbol{d}_i$ be the transmitted symbols of the BS node during DL in the i-th symbol period and N denotes the number of the subcarrier, where,

$$\boldsymbol{d}_i = \left[d_i(0) \quad d_i(1) \quad \cdots \quad d_i(N-1)\right]. \tag{5}$$

As noted in [12], the transmitted symbols are fed to a conventional OFDM modulator that consists of an N-point inverse discrete Fourier transform (IDFT) unit followed by the insertion of an N_g-point cyclic prefix (CP) to avoid interference between adjacent blocks. The output of IDFT unit is denoted as:

$$\boldsymbol{s}_i = \left[s_i(0) \quad s_i(1) \quad \cdots \quad s_i(N-1)\right], \tag{6}$$

where the CP is denoted as:

$$s_i(k) = s_i(k+N) \quad for \quad -N_g \le k \le -1. \tag{7}$$

The modulated symbol on the k-th subcarrier is:

$$s_i(k) = \frac{1}{\sqrt{N}}\sum_{n=0}^{N-1} d_i(n) e^{\frac{j2\pi nk}{N}} \quad \text{for } -N_g \le k \le N-1\,. \tag{8}$$

The discrete-time downlink signal takes the form:

$$s^T(k) = \sum_i s_i(k - iN_T)\,, \tag{9}$$

where $N_T = N + N_g$.

By considering the time-variant frequency-selective fading channel between BS and MS, we denote the channel impulse response (CIR) of the l-th subcarriers as $h(l)$ and $l \in \{0,1,\cdots,L-1\}$. The received signal on the k-th subcarriers of MS in the i-th symbol period is:

$$r_i(k) = P_{BS}\sum_{l=0}^{L-1} h(l)s_i(l) + w(k), \quad (10)$$

where P_{BS} is the transmission power of BS, and $w(k)$ is the complex-valued additive white Gaussian noise (AWGN). The received signal of MS during contiguous symbol period is:

$$r(k) = P_{BS}\sum_i \sum_{l=0}^{L-1} h(l)s_i(k-l-iN_T) + w(k). \quad (11)$$

At the receiver, $r(k)$ is divided into adjacent segments of length N_T, each corresponding to a transmitted OFDMA block. Assuming the CP is longer than the CIR duration, after removing the CP, the remaining N samples are passed to an N-point discrete Fourier transform (DFT) unit, and the output of the DFT unit is:

$$R_{i,n} = P_{BS}H_n d_{i,n} + w_{i,n}, \quad (12)$$

where

$$H_n = \sum_{l=0}^{L-1} h(l)e^{-\frac{j2\pi nl}{N}}, \quad (13)$$

and $w_{i,n}$ is the equivalent additive noise after DFT, which is with the complex Gaussian distribution.

By considering the frequency shift in AFAIC case calculated in (2), ε is less than the bandwidth of the subcarrier, the frequency shift only leads to the intersubcarrier interference. The received signal of the MS in (10) can be rewritten as:

$$R_{i,n} = P_{BS}e^{j\varphi_i}H_n f_N(\varepsilon)d_{i,n} + I_{i,n}(\varepsilon) + w_{i,n}. \quad (14)$$

Where

$$\varphi_i = \frac{2\pi\varepsilon_i N_T}{N}, \quad (15)$$

$$f_N(\varepsilon) = \frac{\sin(\pi\varepsilon)}{N\sin\left(\frac{\pi\varepsilon}{N}\right)}e^{\frac{j\pi\varepsilon(N-1)}{N}}, \quad (16)$$

and $I_{i,n}(\varepsilon)$ denotes the interference signal caused by the adjacent subcarriers. Since $I_{i,n}(\varepsilon)$ relates to the transmitted symbols on the adjacent subcarriers, we model it as a zero-mean random variable with its power denoted as

$$\sigma_I^2(\varepsilon) = P_{BS}\left[1 - \left|f_N(\varepsilon)\right|^2\right]. \quad (17)$$

By considering the Rice channel model of the AFAIC case in (3), formula (14) can be rewritten as:

$$\begin{aligned} R_{i,n} &= P_{BS}ae^{j\varphi_i}f_N(\varepsilon)d_{i,n} \\ &+ \sum_{l=0}^{N-1} P_{BS}ce^{\varphi_i}h(l)e^{-\frac{j2\pi nl}{N}}f_N(\varepsilon)d_{i,n}. \\ &+ I_{i,n}(\varepsilon) + w_{i,n} \end{aligned} \quad (18)$$

During the UL transmission of AeroMACS, the flexible OFDMA spectrum allocation schemes are allowed. Normally, there are two UL transmission cases.

The first case is that in one symbol period, all the subcarriers are allocated to one MS node, and this scheme befits for the case that there are small number of MS nodes in the coverage zone of BS. The transmission model is similar with the DL mode. This scheme does not fit in the AG and the AHTR cases since large number of MS nodes results in lower spectrum allocation efficiency and more time delay.

Another case is that in one symbol period, the subcarriers are allocated to u MS nodes (MS_1,MS_2,…, MS_u), and we assume that the N_{us}-th to the N_{ue}-th subcarriers are allocated to the u-th MS. After IDFT, the modulated signal of the u-th MS at the k-th subcarrier is:

$$s_{i,u}(k) = \frac{1}{\sqrt{N}}\sum_{n=N_{us}}^{N_{ue}-1} d_{i,u,n}e^{\frac{j2\pi nk}{N}}, \quad \text{for } -N_{us} \le k \le N_{ue}-1 \quad (19)$$

The received signal at the k-th subcarrier of BS can be denoted as:

$$r_i(k) = \sum_{u=0}^{U-1} P_u \sum_{k=N_{u1}}^{N_{u2}-1} h_u(k)s_{i,u}(k) + w_i(k), \quad (20)$$

where $h_u(k)$ is the CIR of the channel from MS_u to BS on the k-th subcarrier. The demodulated signal after DFT at BS node is:

$$R_{i,n} = \sum_{u=0}^{U-1} P_u \sum_{k=N_{us}}^{N_{ue}-1} h_u(k)e^{-\frac{j2\pi nk}{N}}d_{i,u}(k) + w_{i,n}. \quad (21)$$

Let,

$$H'_{n,u} = \sum_{k=N_{us}}^{N_{ue}-1} h_u(k)e^{-\frac{j2\pi nk}{N}}d_{i,u}(k), \quad (22)$$

and ε_u be the nominalized frequency shift of the u-th MS, the received signal at the MS can be described as:

$$R_{i,n} = \sum_{u=0}^{U-1} P_u e^{j\varphi_{i,u}} f_N(\varepsilon_u)H'_{n,u}d_{i,u}(k) + I_{i,n}(\varepsilon_u) + w_{i,n}. \quad (23)$$

By considering the Rice channel model in (3), formula (23) can be rewritten as":

$$\begin{aligned} R_{i,n} &= \sum_{u=0}^{U-1} a_u P_u e^{j\varphi_{i,u}} f_N(\varepsilon_u)d_{i,u}(k) \\ &+ \sum_{u=0}^{U-1}\sum_{k=N_{us}}^{N_{ue}-1} c_u P_u e^{\varphi_i}h_u(k)e^{-\frac{j2\pi nk}{N}}f_N(\varepsilon_u)d_{i,u}(k). \\ &+ \sum_{u=0}^{U-1} I_{i,n}(\varepsilon_u) + w_{i,n} \end{aligned} \quad (24)$$

A dramatic phenomenon is that, in the AFAIC case, the aircrafts are with the similar approaching speeds and the climbing speeds. The frequency shifts of different MS nodes are with the similar values.

During the decoding process at the receiver, we propose a rough CIR estimation and decoding (RCED) scheme. In this scheme, we estimate the affected CIR instead of the parameter ε by one precursor symbol. Then, the receiver treats the interference signal $I_{i,n}(\varepsilon)$ as the additional noise. The process of RCED scheme is similar

with the normal decoding process, which can run under the IEEE 802.16e protocol receiver. So the RCED scheme can be realized by the limited improvement of the existing equipment.

In the DL process of AFAIC case, before transmission, we design a precursor symbol vector $\boldsymbol{d}_p$ which is known by the receiver. The precursor symbol is as follows:

$$\boldsymbol{d}_p = \left[\underbrace{1 \quad 1 \quad \cdots \quad 1}_{N} \right]. \tag{25}$$

The modulated symbol on the *k*-th subcarriers is:

$$s_p(k) = \frac{1}{\sqrt{N}} \sum_{n=0}^{N-1} e^{\frac{j2\pi nk}{N}} \quad \text{for} -N_g \le k \le N-1. \tag{26}$$

The received signal of the precursor period at the *n*-th output of DFT unit of MS node is:

$$R_{p,n} = P_{BS} e^{j\varphi_p} H_n f_N(\varepsilon) + I_{i,n}(\varepsilon) + w_{i,n}, \tag{27}$$

Let $T(n) = P_{BS} e^{j\varphi_p} H_n f_N(\varepsilon)$ be the transmission coefficient, it can be estimated during the precursor period as:

$$\hat{T}(n) = \arg\min_{T(n)} \left\{ \left| R_p(n) - T(n) \right| \right\}, \tag{28}$$

which also denoted as the received signal of the precursor slot at the *n*-th output of DFT unit.

The decoding process of the following symbol periods can be described as:

$$\hat{d}(n) = \arg\min_{d(n)\in\Delta} \left\{ \left| R_i(n) - \hat{T}(n) d(n) \right| \right\}, \tag{29}$$

where Δ represents the possible symbol set of the transmitted signals.

The flow diagram of the RCED process is shown in Fig. 4. BS continual transmits one signal packet which includes $\{\boldsymbol{d}_p, \boldsymbol{d}_1, \boldsymbol{d}_2, \cdots, \boldsymbol{d}_I\}$. The packet length, which equals to I+1, depends on the time-variant characteristic of the transmission channel.

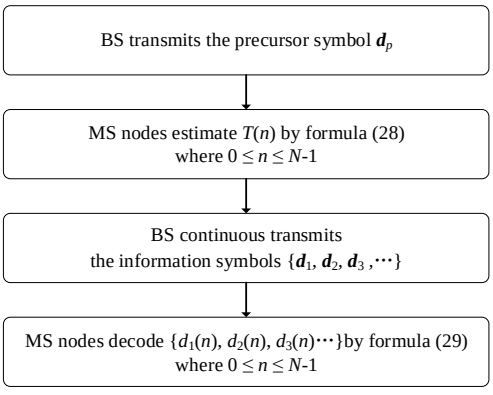

Fig. 4. Flow diagram of the RCED process.

In the UL process, to estimate the transmission coefficient, the known precursor periods are allocated to each MS node, respectively, and the transmission coefficient estimating and the decoding process are similar with the DL case.

IV. PERFORMANCES ANALYSIS

The performances of SNR loss, the spectrum efficiency and BER of the transmission scheme in AFAIC case are discussed in this part, and to simplify the analysis process, the DL transmission is considered.

Let SNR_{real} be the real SNR of the receiver at MS, and the channel gain is equalized, the real SNR is:

$$SNR_{\text{real}} = \frac{P_{BS} E\left\{ \left| f_N(\varepsilon) \exp^{j\varphi_i} \right|^2 \right\}}{\sigma_I^2(\varepsilon) + \sigma_w^2}, \tag{30}$$

where P_{BS} is the transmission power of the BS, $E\left\{ \left| f_N(\varepsilon) \exp^{j\varphi_i} \right|^2 \right\}$ is the coefficient of the transmitted signal, which represents the effect of the frequency shift of the signal, $\sigma_I^2(\varepsilon)$ and σ_w^2 are the power of the interference signal and the AWGN, respectively.

With the increase of the speed of MS node, the power of the signal, which equals to the primal signal power multiplied by the coefficient $E\left\{ \left| f_N(\varepsilon) \exp^{j\varphi_i} \right|^2 \right\}$, reduces and the power of intersubcarrier interference, which equals to $P_{BS}\left[1 - \left| f_N(\varepsilon) \right|^2\right]$, increases.

According to the typical AeroMACS system in [2], we assume that the FFT point is 512, the symbol period is 1.75×10^{-7} seconds, and N_g equals 64 (1/8 symbol period).

Without loss of generality, AWGN is assumed as a complex random variable, the mean and variance equal 0 and 1, respectively. Since the power of AWGN can be recognized as the variance of it, we set $\sigma_w^2 = 1$.

Let $SNR_{\text{sync}} = P_{BS} / \sigma_w^2$ be the ideal SNR of the synchronic communication system. Performances of SNR loss in AFAIC case with different SNR_{sync} values, i.e., 5dB, 10dB, 15dB, 20dB and 30dB, are shown in Fig. 5.

In the case that SNR_{sync} is low, which means that MS is far away from BS, the real SNR loss is small. When SNR_{sync} =5dB , the SNR loss is about 1dB for the case that the MS node moves at 400 km/h.

With the increase of SNR_{sync}, which indicates that the MS approaches BS, the influence of Doppler frequency shift is obvious. When the speed of MS is 250km/h, which is the most common approaching speed and the initial climbing speed of civil aircraft, the real SNR loss are 2dB, 7dB and 16dB in the case that SNR_{sync} equal 10 dB, 20 dB and 30 dB, respectively. For the case that the speed of MS is 400km/h, SNR_{real} reduces to less than 10dB.

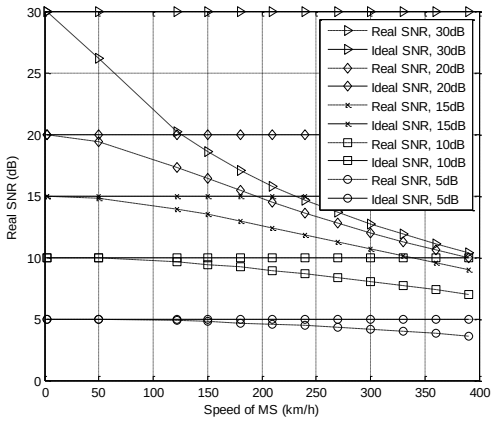

Fig. 5. SNR loss in AFAIC case, where SNR_{sync} is set to 5dB, 10dB, 15dB, 20dB and 30dB, and different move speeds of MS node are considered.

Simulation results of spectrum efficiency under different moving speeds of MS node are shown in Fig. 6. By considering that different modulation scheme will cause varying transmission performance, four common modulation schemes, i.e., binary phase shift keying (BPSK), quadrature phase shift keying(BPSK), 16-quadrature amplitude modulation(QAM) and 64-QAM are considered. Since the channel gain is equalized, the gain of LOS path does not affect the simulation results.

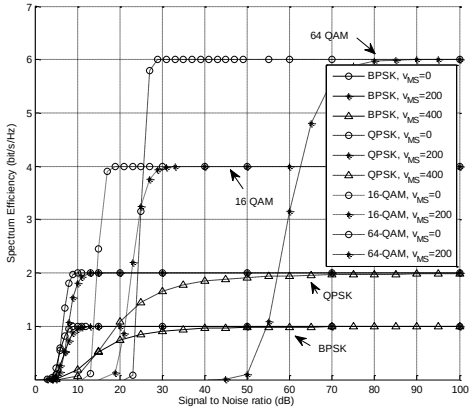

Fig. 6. Spectrum efficiency for BPSK, QPSK, 16-QAM and 64-QAM with different moving speed of MS node.

For the BPSK modulation, to reach half spectrum efficiency (0.5 bit/s/Hz), SNR_{sync} are 5dB, 7dB and 15dB for the speed of MS are 0km/h, 200km/h and 400km/h, respectively. For the QPSK modulation, to reach half spectrum efficiency (1 bit/s/Hz), SNR_{sync} are 6dB, 8dB and 20dB for the speed of MS are 0km/h, 200km/h and 400km/h, respectively.

For the 16-QAM modulation, to reach the half spectrum efficiency point (2 bit/s/Hz), SNR_{sync} are 14dB and 23dB for the speed of MS are 0km/h and 200km/h, respectively. For the 64-QAM modulation scheme case, to reach the half spectrum efficiency point (3 bit/s/Hz), SNR_{sync} are 25dB and 60dB for the speed of MS are 0km/h and 200km/h, respectively. For 16-QAM and 64-QAM modulation schemes, SNR_{sync} should be more than 100dB to reach the half spectrum efficiency in the case that the speed of MS is 400 km/h, which is not realistic in AeroMACS.

From the results, the spectrum efficiency loss of the higher order modulation scheme (i.e., 16-QAM and 64-QAM) is greater than the lower cases. The reason of huge spectrum efficiency loss in the high order modulation cases is that the high order modulated code is with smaller Euclidean distance, which is much easier to be affected by the interference signal and the AWGN.

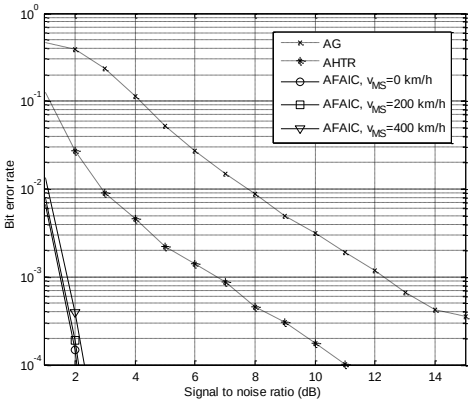

Fig. 7. BER performances of BPSK modulation.

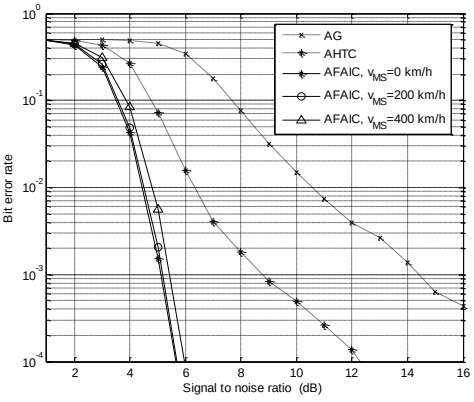

Fig. 8. BER performances of QPSK modulation.

BER performances of the abovementioned 4 modulation schemes are shown in Fig. 7 to Fig. 10, and the K_{RICE} is set to 15dB as the typical value in AFAIC case.

For BPSK and QPSK modulations, as shown in Fig.

7 and Fig. 8, when the moving speed of MS is 200km/h, the BER performances are similar with the case that MS node is stationary. In the case that the moving speed of MS reaches 400km/h, the BER performance loss is less than 0.5dB, which means that the proposed scheme can fit the AFAIC case for the low order modulation schemes.

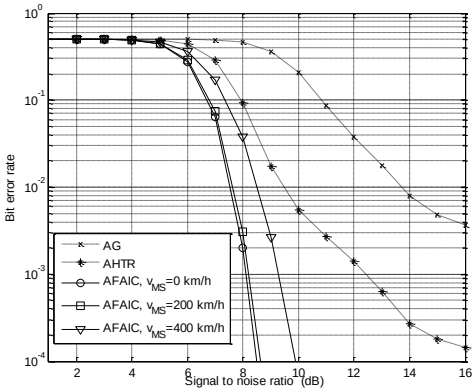

Fig. 9. BER performances of 16-QAM modulation.

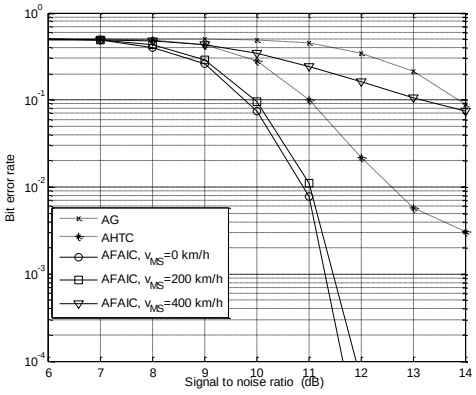

Fig. 10. BER performances of 64-QAM modulation.

As shown in Fig. 9, for 16-QAM modulation, compared with the case that MS node is stationary, the BER performance loss are 0.1dB and 1.5dB for the case that the moving speed of MS are 200km/h and 400km/h, respectively.

For 64-QAM modulation shown in Fig. 10, the BER performance loss is about 0.3dB for the case that the moving speed of MS is 200km/h. When the moving speed of MS is 400km/h, BER performance is with significant loss. The BER only reaches 10^{-1} when SNR is 14dB.

We also show the BER performances in the AG case and the AHTR case where K_{RICE} are set to 0 and 6.7dB, respectively [19]. Benefit from the strong gain of LOS path in AFAIC case, BER performances of BPSK, QPSK and 16-QAM modulation schemes in the AFAIC case with the moving speed of MS is 400km/h are better than the AG case and AHTR case significantly. For the 64-QAM modulation, the BER performance of the 400km/h moving speed case is with mightily loss, which is worse than the AHTR case and reaches the same BER with the AG case when SNR reaches 14dB.

Summarizing the simulation results in Fig. 5 to Fig. 10, we can get the transmission characteristics in AFAIC case. Firstly, the interference caused by the high moving speed of MS seriously affects the real SNR and the transmission efficiency, however, this interference signal is difficult to be cancelled. Secondly, the strong LOS path of the channel in AFAIC case can provide a stable transmission environment between BS and MS nodes, which can reduce BER of the transmission system. Third, increase the modulation order will lead to a sharp increase in BER. By using lower order modulation, the proposed RCED scheme can meet the communication requirements of AeroMACS in AFAIC case.

V. CONCLUSION

In this paper, to combat the Doppler frequency shift in AFAIC case, we propose a RCED scheme which estimates the affected CIR instead of the nominalized frequency shift at the receiver. It can run under the IEEE 802.16e protocol receiver, which can be realized by the limited improvement of the existing equipment. Simulation results of BER performance show that the proposed RCED scheme can meet the requirements of AeroMACS. From our research, the coverage zone of AeroMACS can be expanded from the ground part (which include the AG case and the AHTR case) to the takeoff and approaching strip (the AFAIC case), which is benefit to improve the ATM communication link. The data of aircrafts in approaching can also be used to estimate the grounding point and grounding time, which provides data support for guidance, collision avoidance and path planning of ground vehicles in the A-SMGCS.

ACKNOWLEDGMENT

This work was supported by the Research project of Tianjin education commission (No. 2018KJ239) and the open fund of Tianjin key lab for advanced signal processing (No. 2017ASP-TJ02).

REFERENCES

[1] Eurocontrol and FAA, COCRv2, *Communications Operating Concept and Requirements for the Future Radio System*, 2007.

[2] G. Bartoli, R. Fantacci, and D. Marabissi, "AeroMACS: A new perspective for mobile airport communications and Services," *IEEE Wireless Communications*, vol. 20, pp. 44-50, Dec 2013.

[3] C. Brian, "Service considerations for an AeroMACS

network reference model: Delivering next generation communications to the airport surface," *2015 Integrated Communication, Navigation, and Surveillance Conference (ICNS) IEEE*, pp. 1-21, June 2015.

[4] B. Giulio, et al., "An efficient subcarrier allocation method for AeroMACS-Based communication systems," *IEEE Transactions on Aerospace and Electronic Systems*, vol. 49, no. 2, pp. 786-797, Apr. 2013.

[5] O. Mohammad, O. Nasser, and G. Noradin, "Enhanced bandwidth small square slot antenna with circular polarization characteristics for WLAN/ WiMAX and C-band applications," *Applied Computational Electromagnetics Society Journal*, vol. 28, no. 2, pp. 156-161, Feb. 2014.

[6] R. Vahid, S. Hasan, and K. Saeid, "Circularly polarized aperture-coupled microstrip-line fed array antenna for WiMAX/ C bands applications," *Applied Computational Electromagnetics Society Journal*, vol. 32, no. 12, pp. 1117-1120, Dec. 2017.

[7] K. Morioka, et al., "EVM and BER evaluation of C band new Airport surface communication systems," *International Workshop on Antenna Technology: small Antennas, Novel Em Structures and Materials, and Applications IEEE*, Sydney, pp. 242-245, Mar. 2014.

[8] C. Antonio and N. Fistas, "AeroMACS: Impact of link symmetry on network capacity," *2016 Integrated Communications Navigation and Surveillance (ICNS) IEEE*, Piscataway, NJ, pp. 1-9, Apr. 2016.

[9] N. Kanada, et al., "MIMO effect evaluation for aeronautical WiMAX in airport at 5.1GHz," *Integrated Communications, Navigation & Surveillance Conference IEEE*, pp. 1-10, Apr. 2012.

[10] N. Kanada, et al., "Evaluation of antenna configuration for aeronautical WiMAX at 5.1GHz," *Wireless & Microwave Technology Conference IEEE*, pp. 1-4, Apr. 2012.

[11] K. Behnam and R. J. Kerczewski, "IEEE 802.16J multihop relays for AeroMACS networks and the concept of multihop gain," *2013 Integrated Communications, Navigation and Surveillance Conference (ICNS) IEEE*, Herndon, VA, pp. 1-7, Apr. 2013.

[12] M. Morelli, et al., "Synchronization techniques for orthogonal frequency division multiple access (OFDMA): A tutorial review," *Proceedings of the IEEE*, vol. 95, no. 7, pp. 1394-1427, July 2007.

[13] F. Romano, et al., "Adaptive modulation and coding techniques for OFDMA systems," *IEEE Transactions on Wireless Communications*, vol. 8, no. 9, pp. 4876-4883, Sep. 2009.

[14] M. Michele, L. Marchetti, and M. Moretti, "Maximum likelihood frequency estimation and preamble identification in OFDMA-based WiMAX systems," *IEEE Transactions on Wireless Communications*, vol. 13, no. 3, pp. 1582-1592, Mar. 2014.

[15] A. Biagioni, et al., "Adaptive subcarrier allocation schemes for wireless ODFMA systems in WiMAX networks," *IEEE Journal on Selected Areas in Communications*, vol. 27, no. 2, pp. 217-225, Feb. 2009.

[16] P. Paola, et al., "AeroMACS evolution-analysis during landing, takeoff, and approach phases," *IEEE Transactions on Aerospace and Electronic Systems*, vol. 50, no. 3, pp. 1899-1912, July 2014.

[17] WiMAX Forum Network Architecture — Stage 2: Architecture Tenets, Reference Model and Reference Points, *WIMAX Forum*, Tech. Rep., Feb. 2009.

[18] International Civil Aviation Organization, *Doc 9905: Required Navigation Performance Authorization Required (RNP AR) Procedure Design Manual.*

[19] E. Haas, "Aeronautical channel modeling," *IEEE Transactions on Vehicular Technology*, vol. 51, no. 2, pp. 254-264, Mar. 2002.

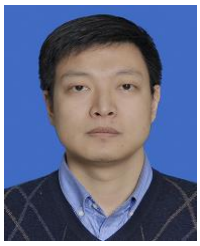

Yuchu Ji received his Ph.D. degree in School of Electronic Information Engineering, Tianjin University, Tianjin, China in 2014. Currently, he is a Lecturer at College of Electronic Information and Automation in Civil Aviation University of China. His research interests include 3 part, wireless sensor network and wireless communication system, cooperative communication, and intelligent airport.

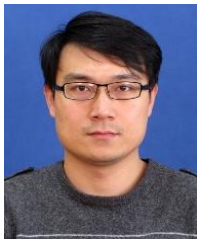

Yang Wang received his Ph.D. degree in Control Science and Engineering from Tianjin University, China in 2013. Currently, he is a Lecturer at Civil Aviation University of China. His research interests include artificial olfaction, mobile robotics and intelligent airport.

Yuan Sang received her master degree in School of Information and Control Engineering from China University of Mining and Technology in 2011. She is a Wireless Communication Engineer and also an Information Technology Engineer in Inventec Group (Tianjin) Electronic Technology Company.